International Journal of Mass Spectrometry 282 (2009) 56–63

Contents lists available at ScienceDirect

International Journal of Mass Spectrometry

journal homepage: www.elsevier.com/locate/ijms

Density functional theory study of $C_nF_3^-$ ($n=1$–9) clusters

J.Y. Qi [a], H. Liang [a], M.D. Chen [a,*], W. Wu [a], Q.E. Zhang [a], C.T. Au [b]

[a] *State Key Laboratory of Physics Chemistry of Solid Surfaces, Department of Chemistry, Center for Theoretical Chemistry, College of Chemistry and Chemical Engineering, Xiamen University, Xiamen 361005, People's Republic of China*

[b] *Department of Chemistry, Hong Kong Baptist University, Kowloon Tong, Hong Kong, People's Republic of China*

ARTICLE INFO

Article history:
Received 16 January 2009
Received in revised form 9 February 2009
Accepted 9 February 2009
Available online 20 February 2009

Keywords:
Fluorine-doped anionic carbon clusters
$C_nF_3^-$
Binary cluster anions
Density functional theory study

ABSTRACT

In this paper, we report the design of numerous $C_nF_3^-$ ($n=1$–9) models. By means of B3LYP density functional method, we carried out geometry optimization and calculation on the vibrational frequency. After comparison of structure stability, we found that the structures of ground-state (G-S) isomers of odd-n $C_nF_3^-$ (i.e., $n=3$, 5, 7 and 9) are with the three fluorine atoms located at one end of the linear C_n chain. The G-S isomers of $C_2F_3^-$, $C_4F_3^-$, and $C_8F_3^-$ are with two fluorine atoms bonded to an end carbon of the C_n chain, and one fluorine atom bonded to the adjacent carbon atom. In other words, the two carbon atoms involved in bonding to the fluorine atoms are *sp*^{2} hybridized and the C_n chain is not linear. In the case of $C_6F_3^-$, the G-S isomer is planar cyclic in structure, with each of the three carbon atoms at one side of the hexagonal C_6 ring bonded to a fluorine atom. The C_n chain of G-S $C_nF_3^-$ ($n=3$–9; $C_6F_3^-$ being the exception) isomers are polyacetylene-like. It is found that the odd-n G-S $C_nF_3^-$ ($n=1$–9) are more stable than the adjacent even-n ones. The finding is in accord with the relative intensities of $C_nF_3^-$observed in mass spectrometric studies. We provide explanations for such trend of even/odd alternation based on concepts of the geometrical structure, bonding character, atomic charges, vertical electron detachment energy, and incremental binding energy.

1. Introduction

In the past decades, carbon clusters have been studied experimentally as well as theoretically. Even before the development of fullerene chemistry, small carbon clusters were studied due to their importance in combustion and pyrolysis, in formation and growth of fullerenes and nanotubes, and in astrophysical processes related to the identification of species in interstellar and circumstellar media [1,2]. In outer space under quasi-collisionless conditions, carbon takes the highly stable, albeit highly reactive, form of linear chains in which the atomic orbitals are *sp* hybridized [3]. In recent years, the doping of carbon clusters with heteroatom(s) has received much attention because the addition of heteroatom(s) provides a means to stabilize the carbon chain. The study of anionic clusters is of particular interest because method such as photoelectron spectroscopy can only provide indirect information related to the structures of these materials [4]. By means of secondary ionic emission or laser ionization, C_nX^- clusters ($X=$ an atom of main group, transition or non-metal element) can be fabricated [5–9]. As for fluorine-doped carbon clusters, $C_nF_m^-$ species were detected experimentally by Gnaser when a teflon specimen was sputtered in a standard secondary-ion mass spectrometer investigation [10].

Numerous theoretical studies on C_nX^- (X being an element other than carbon) clusters have been conducted by various research groups using different levels of calculation. Zheng and coworkers studied C_nN^- ($n=1$–13) [11], C_nB^- ($n=1<13$) [12], C_nP^- ($n=1$–13) [13], AlC_n^- ($n=1$–11) [14], and C_nSe^- ($1\leq n\leq 11$) [15] clusters by means of HF/3-21G level or B3LYP/6-31G* density functional method. Zhan and Iwata reinvestigated C_nN^- ($n=1$–13) [16], C_nB^- ($n=1$–7) [17] and C_nP^- ($n=1$–7) [18] using methods of ab initio approximation. Pascoli and Lavendy proposed structures of C_nN^- ($n=1$–7) [19] and C_nP^- ($n=1$–7) [20] based on data collected in B3LYP/6-311G* density functional calculation. Fisher et al. conducted BLYP density functional calculations on structures of C_nP^- ($n=3$–9) [21]. Tang and coworkers carried out a comparative study on linear ground-state (denoted as G-S hereinafter) carbon clusters C_nX^- ($n=1$–10, $X=$ Na, Mg, Al, Si, P, S or Cl) [22], PbC_n^- ($n=1$–10) [23] and GeC_n^- ($n=1$–9) [24] by means of DFT/B3LYP method. Vandenbosch and Will analyzed RbC_n^- ($n=1$–10) [25] clusters by ab initio method. Hunsicker and Jones performed density functional calculations with annealing simulation on $Si_nC_m^-$ ($n+m\leq 8$) [26]. Gomei et al. investigated various SiC_n^- ($n=2$–5) anions by ab initio molecular orbital approach [27]. Pan et al. studied C_nH^- ($n\leq 10$) based on density functional calculations [28]. Using density functional method, Largo and coworkers conducted researches on AlC_n^- ($n=1$–7) [29], NaC_n^- ($n=1$–8) [30], MgC_n^- ($n=1$–7) [31,32], CaC_n^- ($n=1$–8) [33], C_nCl^- ($n=1$–7) [34], TiC_n^- ($n=1$–8) [35], and VC_n^- ($n=1$–8) [36]. Zhai et al. performed study on CrC_n^- ($n=2$–8) by

---

[*] Corresponding author. Tel.: +86 592 2182332; fax: +86 592 2184708.
E-mail address: mdchen@xmu.edu.cn (M.D. Chen).

1387-3806/$ – see front matter © 2009 Elsevier B.V. All rights reserved.
doi:10.1016/j.ijms.2009.02.007

density functional method [37]. We carried out density functional study on the structures and energies of C_nAs^- (n = 1–11) [38], BeC_n^- (n = 1–8) clusters [39] and CsC_n^- (n = 1–10) clusters [40].

Until now there is no theoretical investigation on fluorine-doped carbon anions. In the generation of clusters of fluorine-carbon anions $C_nF_m^-$, Gnaser observed an odd/even pattern: the intensities of odd-n species are distinctly larger than those of even-n ones [10]. To explore the experimental observation and to explain this striking effect, we designed a large number of structural models of $C_nF_3^-$ (n = 1–9) and performed geometry optimization and calculation on vibrational frequencies by means of the B3LYP density functional method. The geometrical structure, bonding character, atomic charges, vertical electron detachment energy, and incremental binding energy of the clusters were examined. Based on the results, we provide an explanation to why the odd-n G-S $C_nF_3^-$ (n = 1–9) isomers are more stable than the even-n ones. The outcome can serve as a guideline for the synthesis of related materials as well as for future theoretical studies of carbon/fluorine binary clusters.

2. Computational method

The approach adopted in this study has been described elsewhere [41]. Briefly speaking, devices for molecular graphics, molecular mechanics, and quantum chemistry examination were used. First, a three-dimensional model of a cluster was designed using HyperChem for Windows on a PC computer [42]; the model was then optimized by MM+ molecular mechanics and PM3 semi-empirical quantum chemistry. At the final stage, geometry optimization and calculation of vibrational frequencies were conducted using the B3LYP density functional method of Gaussian 03 package [43]; i.e., Becke's 3-parameter nonlocal exchange functional with the correlation functional of Lee–Yang–Parr [44,45]. The single point energy calculations following the optimizations were performed using the larger 6-311+G* basis set, including diffuse functions (i.e., B3LYP/6-311+G*//B3LYP/6-311G*) [46]. It has been pointed out that the common practice of running a high-level single point energy calculation at a geometry computed with a cheaper method is just as good than performing all calculations at the higher level of theory. Using geometries computed with more expensive models (include diffuse function) do not necessarily lead to more accurate final results [32,47]. All energies were calculated with zero point energy (ZPE) correction; as the quality of employed method for calculation has very little effect on ZPE variation, all energies were calculated with ZPE correction at B3LYP/6–311G* level. The optimized models were again displayed using HyperChem. The data of partial charges were analyzed with Gaussian Natural Bond Orbital (NBO). All the calculations were carried out on SGI servers.

3. Results and discussion

3.1. Model structures

Since the possible structures of clusters could be many, it is sensible to identify the G-S ones. At the beginning of the study, nothing was known other than the $C_nF_3^-$ formula. The assumption of a reasonable geometrical structure was the beginning of the optimization process. In order to reduce the chance of having the G-S structures wrongly identified, we examined a huge number of models with various configurations. There are four major configurations adopted by G-S isomers of carbon clusters doped with a single heteroatom: (1) the linear configurations terminated by the heteroatom, e.g., C_nN^- (n = 1–7) [19]. (2) The linear configuration with the heteroatom located inside the C_n chain, e.g., C_nB (n = 4–10) [48]. (3) The configurations with a bent C_n chain terminated by the heteroatom atom, e.g., C_nH^- ($n \leq 10$) [28]. (4) The configurations with the heteroatom lightly embraced by the carbon clusters, e.g., CsC_n^- (n = 1–10) [35,40,49]. In the fluorination of carbon clusters, the number of isomers doped with three fluorine atoms is higher than that doped with one fluorine atom. In the investigation of $C_nF_3^-$ clusters, we mainly considered models that are chain, cyclic, branched, cyclic-branched, and shared cyclic in structure.

The adopted approach for the determination of geometries is based on comparison of total energies. After geometry optimization, the total energies were compared for the determination of G-S isomers. Shown in Figs. 1–5 are the $C_nF_3^-$ (n = 1–9) isomers

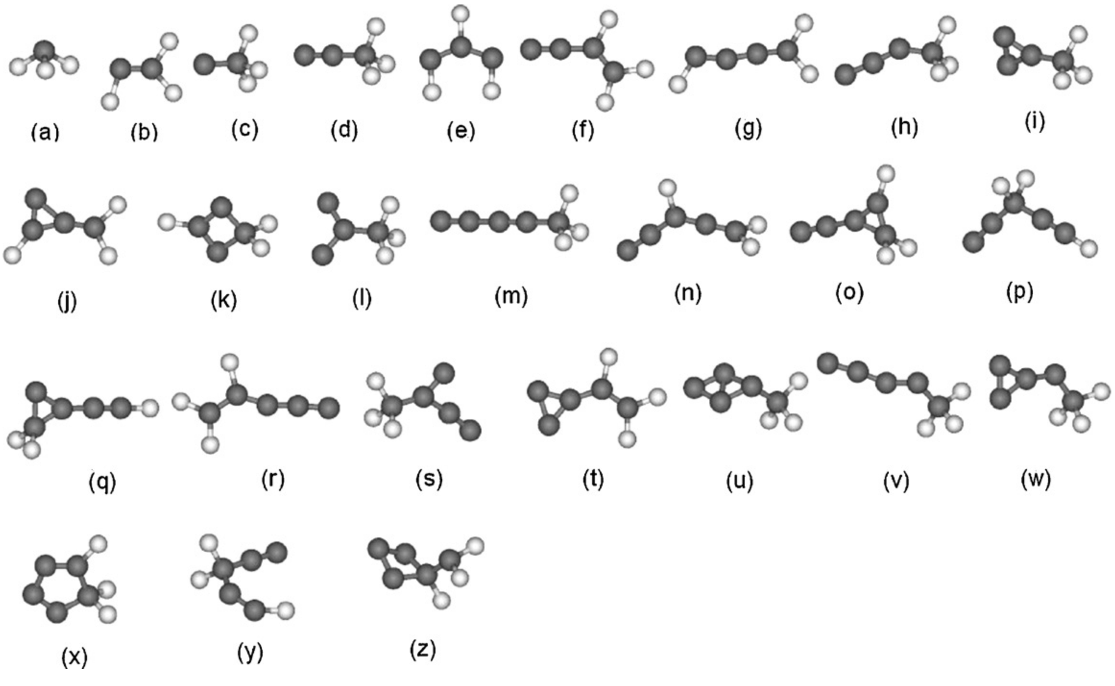

Fig. 1. Twenty-six isomers of $C_nF_3^-$ (n = 1–5).

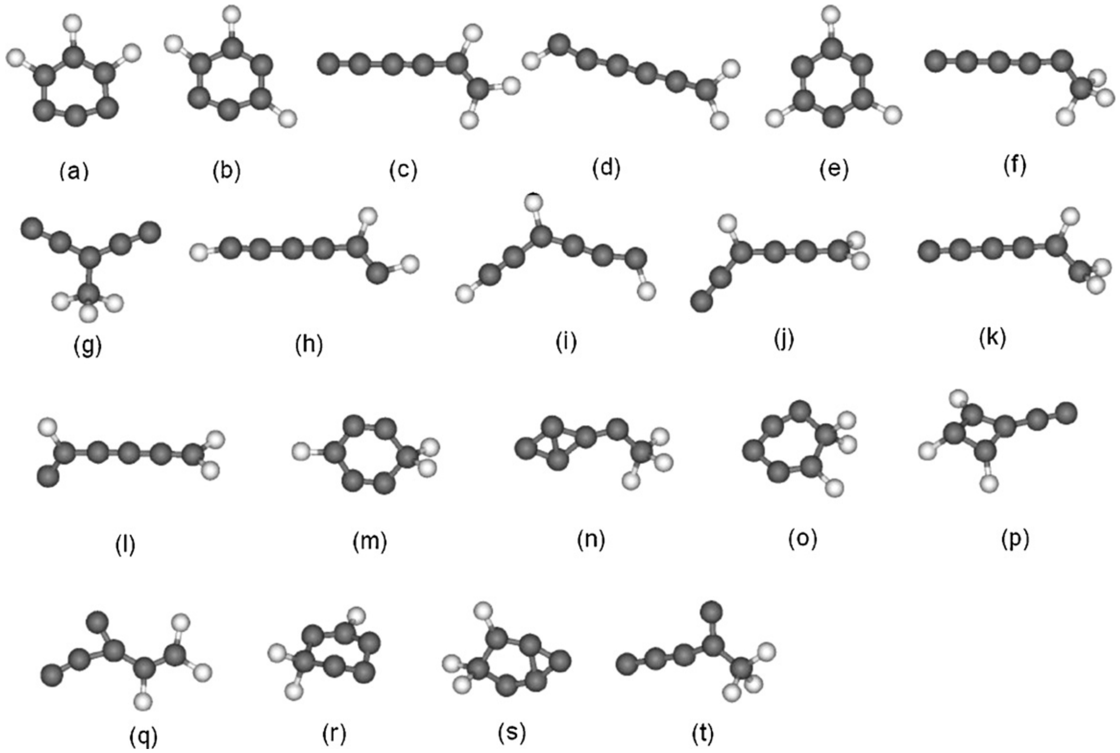

Fig. 2. Twenty isomers of $C_6F_3^-$.

corresponding to local minima with real vibrational frequencies. For the models of a particular n, they are arranged in the order of ascending total energy. In the figures, dark gray (bigger) balls represent carbon atoms and light gray (smaller) ones denote fluorine atoms. The 26 isomers of $C_nF_3^-$ ($n = 1$–5) acquired are shown in Fig. 1: one for CF_3^- (Model 1a), 2 for $C_2F_3^-$ (Models 1b and 1c), 2 for $C_3F_3^-$ (Models 1d and 1e), 7 for $C_4F_3^-$ (Models 1f–ll), and 14 for $C_5F_3^-$ (Models 1m–1z). If the number of isomers acquired for a particular n is more than 20, only the "low-energy" 20 would be depicted in this paper. We obtained a total of 34 isomers of $C_6F_3^-$, and depicted only the "low-energy" 20 (Models 2a–2t) in Fig. 2. Shown in Fig. 3 are 20 $C_7F_3^-$ isomers (Models 3a–3t). Depicted in Fig. 4 are 20 "low-energy" isomers of $C_8F_3^-$ (Models 4a–4t) out of a total of 30 obtained isomers. Depicted in Fig. 5 are 20 "low-energy" isomers of $C_9F_3^-$ (Models 5a–5t) out of a total of 45 acquired isomers. As far as we know, none of these models have been reported before.

Listed in Table 1 are the symmetry, electronic state, total energy, and relative energy of the $C_nF_3^-$ ($n = 1$–6) structures displayed in Figs. 1 and 2. Similar data of the $C_nF_3^-$ ($n = 7$–9) structures displayed in Figs. 3–5 are listed in Table 2.

According to the relative energies shown in Tables 1 and 2, the G-S isomer of CF_3^- adopts a single pyramidal structure whereas that of $C_2F_3^-$ a planar configuration. In the latter case, the two

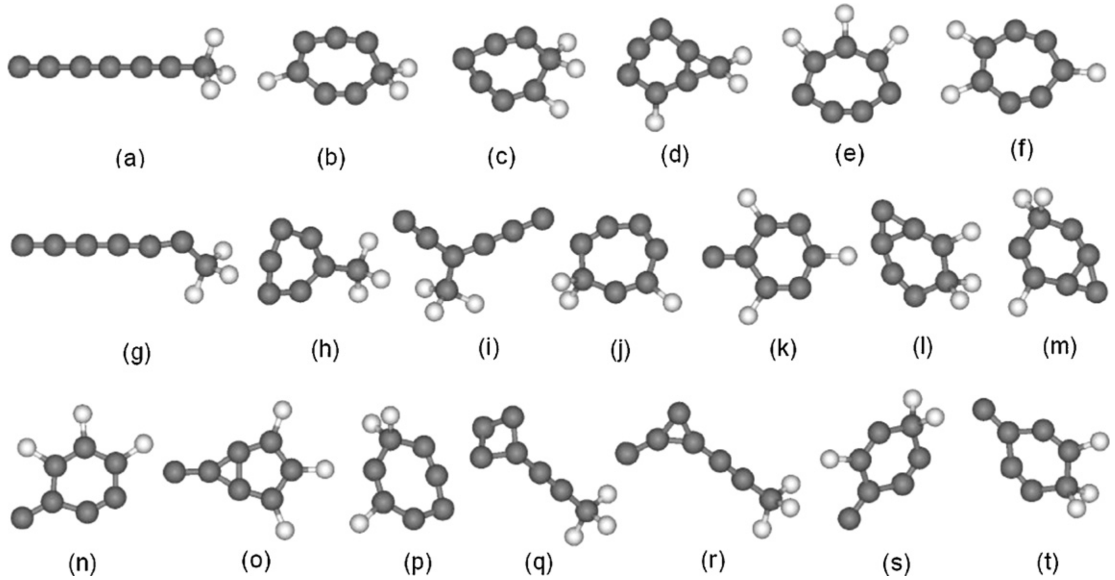

Fig. 3. Twenty isomers of $C_7F_3^-$.

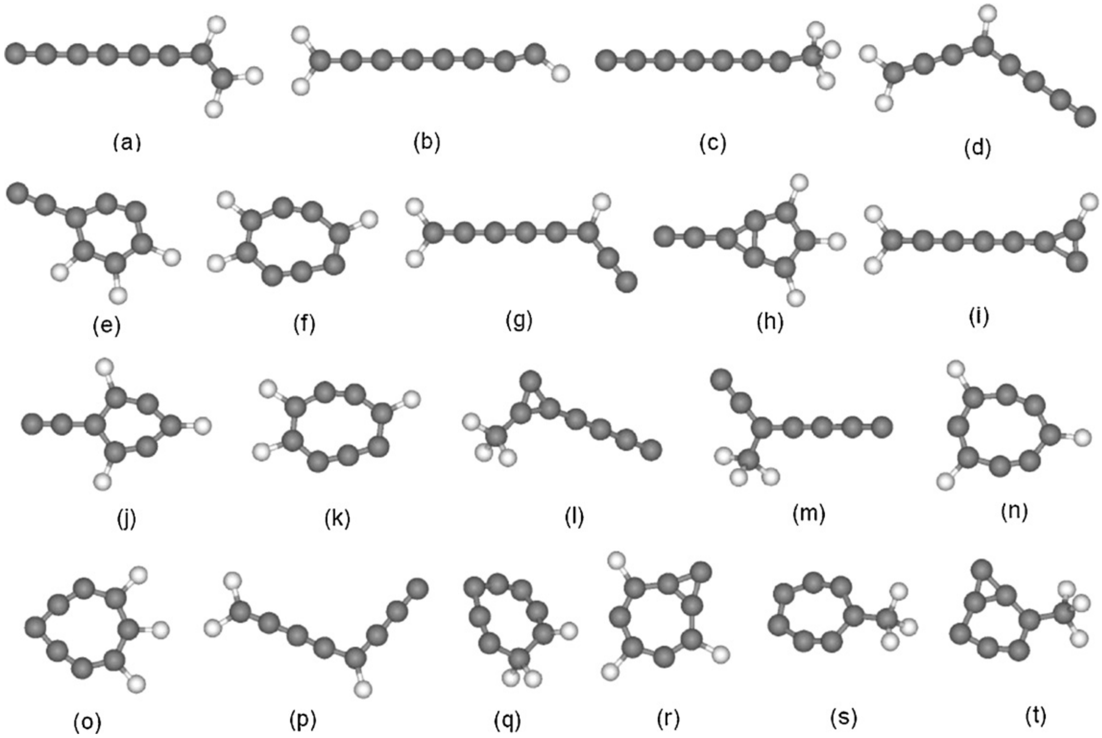

Fig. 4. Twenty isomers of $C_8F_3^-$.

carbon atoms are sp^2 hybridized, forming a C═C double bond; one of the two carbon atoms is connected to two fluorine atoms and the other to one fluorine atom. For the G-S isomers of $C_nF_3^-$ ($n = 3–9$) with that of $C_6F_3^-$ being the only exception, we see chain structures. When n is odd, C_n is linear and the three fluorine atoms are bonded to an end carbon, forming a pyramidal CF_3 unit. When n is even, the C_n chain is bent, displaying a C_2F_3 unit having configuration similar to that of G-S $C_2F_3^-$ (Model 1b) at one end. In the

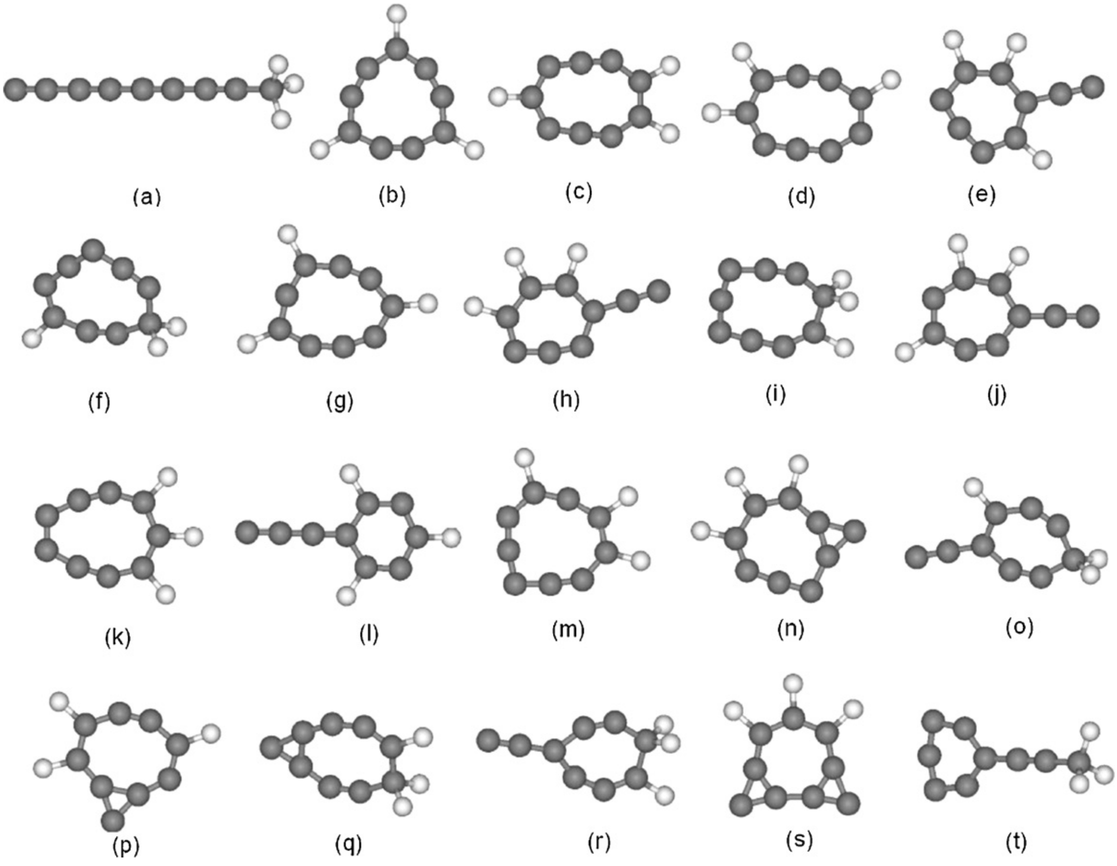

Fig. 5. Twenty isomers of $C_9F_3^-$.

Table 1
Symmetry, electronic state, total energy (a.u.), and relative energy (kcal/mol) of $C_nF_3^-$ (n = 1–6).

Model	Anion	Symmetry	State	Total energy	Relative energy	Model	Anion	Symmetry	State	Total energy	Relative energy
1a	CF_3^-	C_{3v}	$^1A_1$	−337.731034	0.00	1x	$C_5F_3^-$	C_1	^3A	−489.961069	75.48
1b	$C_2F_3^-$	C_s	$^1A'$	−375.786010	0.00	1y	$C_5F_3^-$	C_s	$^3A'$	−489.960742	75.82
1c	$C_2F_3^-$	C_{3v}	$^3A_1$	−375.733675	32.84	1z	$C_5F_3^-$	C_s	$^3A'$	−489.921171	100.31
1d	$C_3F_3^-$	C_{3v}	$^1A_1$	−413.906808	0.00	2a	$C_6F_3^-$	C_{2v}	$^1A_1$	−528.163411	0.00
1e	$C_3F_3^-$	C_s	$^1A'$	−413.823017	52.58	2b	$C_6F_3^-$	C_s	$^1A'$	−528.153788	6.04
1f	$C_4F_3^-$	C_s	$^1A'$	−451.965960	0.00	2c	$C_6F_3^-$	C_s	$^1A'$	−528.143706	12.36
1g	$C_4F_3^-$	C_s	$^1A'$	−451.957927	5.04	2d	$C_6F_3^-$	C_s	$^1A'$	−528.135812	17.32
1h	$C_4F_3^-$	C_s	$^3A''$	−451.937669	17.75	2e	$C_6F_3^-$	C_{3v}	$^3A_1$	−528.131310	20.14
1i	$C_4F_3^-$	C_s	$^1A'$	−451.934545	19.71	2f	$C_6F_3^-$	C_s	$^1A'$	−528.119036	27.85
1j	$C_4F_3^-$	C_s	$^1A'$	−451.934221	19.92	2g	$C_6F_3^-$	C_s	$^1A'$	−528.103647	37.50
1k	$C_4F_3^-$	C_{2v}	$^3B_1$	−451.900682	40.96	2h	$C_6F_3^-$	C_1	^1A	−528.099212	40.29
1l	$C_4F_3^-$	C_s	$^3A''$	−451.847441	74.37	2i	$C_6F_3^-$	C_1	^1A	−528.094318	43.36
1m	$C_5F_3^-$	C_{3v}	$^1A_1$	−490.081032	0.00	2j	$C_6F_3^-$	C_s	$^3A''$	−528.093558	43.83
1n	$C_5F_3^-$	C_s	$^1A'$	−490.049274	19.93	2k	$C_6F_3^-$	C_s	$^3A''$	−528.091021	45.43
1o	$C_5F_3^-$	C_1	^1A	−490.030905	31.46	2l	$C_6F_3^-$	C_s	$^3A''$	−528.074074	56.06
1p	$C_5F_3^-$	C_s	$^1A'$	−490.008455	45.54	2m	$C_6F_3^-$	C_s	$^3A''$	−528.065093	61.70
1q	$C_5F_3^-$	C_1	^1A	−490.008262	45.66	2n	$C_6F_3^-$	C_s	$^1A'$	−528.062841	63.11
1r	$C_5F_3^-$	C_1	^3A	−490.008132	45.75	2o	$C_6F_3^-$	C_s	$^3A''$	−528.058605	65.77
1s	$C_5F_3^-$	C_1	^1A	−489.997036	52.71	2p	$C_6F_3^-$	C_s	$^1A'$	−528.058308	65.95
1t	$C_5F_3^-$	C_1	^1A	−489.994962	54.01	2q	$C_6F_3^-$	C_1	^1A	−528.054846	68.13
1u	$C_5F_3^-$	C_s	$^1A'$	−489.983676	61.09	2f	$C_6F_3^-$	C_1	^1A	−528.052968	69.30
1v	$C_5F_3^-$	C_s	$^3A''$	−489.982233	62.00	2s	$C_6F_3^-$	C_1	^1A	−528.043454	75.27
1w	$C_5F_3^-$	C_s	$^3A''$	−489.960202	75.28	2t	$C_6F_3^-$	C_s	$^3A''$	−528.041857	76.28

case of $C_6F_3^-$, a structure with a C_n chain (Model 2c) is not the most stable; it is beat (by 12.36 kcal/mol) by the planar isomer having the three fluorine atoms bonded to one side of a C_6 ring (Model 2a). It is apparent that regardless of C_n geometries, having the fluorine atoms located at terminal positions is preferred for better stability. The energies of the isomers for a particular cluster are determined by the configuration of C_n and the positions of the fluorine atoms.

The previous theoretical C_nX^- studies are on carbon clusters doped with one heteroatom. In the $C_nF_3^-$ (n = 1–9) study, the carbon clusters are doped with three fluorine atoms. When n is odd, the G-S isomers are with an end carbon atom of the C_n chain bonded to the three fluorine atoms, giving a linear C_n chain with a pyramidal CF_3 unit at one end. Such a configuration resembles that of the most stable isomers commonly observed over carbon clusters doped with one heteroatom. When n is even (with the case of $C_6F_3^-$ being the only exception), the C_n chain is bent at one end, displaying a C_2F_3 unit with a C=C double bond; such a configuration has never been reported before for carbon clusters doped with one heteroatom. On the other hand, we find that it is impossible to have the configurations with the fluorine toms located inside the C_n chain or with the fluorine toms lightly embraced by the C_n chain; those are configurations found possible in the studies of carbon clusters doped with one heteroatom.

Table 2
Symmetry, electronic state, total energy (a.u.), and relative energy (kcal/mol) of $C_nF_3^-$ (n = 7–9).

Model	Anion	Symmetry	State	Total Energy	Relative energy	Model	Anion	Symmetry	State	Total energy	Relative energy
3a	$C_7F_3^-$	C_{3v}	$^1A_1$	−566.255565	0.00	4k	$C_8F_3^-$	C_s	$^3A'$	−604.283954	21.85
3b	$C_7F_3^-$	C_s	$^1A'$	−566.213495	24.92	4l	$C_8F_3^-$	C_1	^1A	−604.283234	22.31
3c	$C_7F_3^-$	C_s	$^1A'$	−566.198252	34.49	4m	$C_8F_3^-$	C_1	^1A	−604.277757	25.74
3d	$C_7F_3^-$	C_s	$^1A'$	−566.192845	37.88	4n	$C_8F_3^-$	C_{2v}	$^3B_2$	−604.272312	29.16
3e	$C_7F_3^-$	C_{2v}	$^1A_1$	−566.190731	39.21	4o	$C_8F_3^-$	C_{2v}	$^3B_2$	−604.269120	31.16
3f	$C_7F_3^-$	C_{2v}	$^3B_1$	−566.178785	46.71	4p	$C_8F_3^-$	C_s	$^1A'$	−604.267016	32.48
3g	$C_7F_3^-$	C_s	$^3A''$	−566.177544	47.48	4q	$C_8F_3^-$	C_s	$^1A'$	−604.250745	42.69
3h	$C_7F_3^-$	C_s	$^1A'$	−566.175327	48.88	4r	$C_8F_3^-$	C_s	$^3A''$	−604.246641	45.27
3i	$C_7F_3^-$	C_s	$^1A'$	−566.168942	52.88	4s	$C_8F_3^-$	C_1	^1A	−604.245117	46.23
3j	$C_7F_3^-$	C_s	$^1A'$	−566.169163	52.74	4t	$C_8F_3^-$	C_s	$^3A''$	−604.234940	52.61
3k	$C_7F_3^-$	C_{2v}	$^1A_1$	−566.165958	54.75	5a	$C_9F_3^-$	C_s	$^1A'$	−642.430213	0.00
3l	$C_7F_3^-$	C_s	$^1A'$	−566.165679	54.93	5b	$C_9F_3^-$	D_{3h}	$^1A_1$’	−642.413205	10.67
3m	$C_7F_3^-$	C_s	$^1A'$	−566.148147	65.93	5c	$C_9F_3^-$	C_{2v}	$^3B_1$	−642.387097	27.06
3n	$C_7F_3^-$	C_s	$^3A''$	−566.144220	68.40	5d	$C_9F_3^-$	C_s	$^3A''$	−642.380673	31.09
3o	$C_7F_3^-$	C_{2v}	$^3A_2$	−566.137862	72.39	5e	$C_9F_3^-$	C_s	$^1A'$	−642.380356	31.29
3p	$C_7F_3^-$	C_s	$^3A'$	−566.135567	73.83	5f	$C_9F_3^-$	C_s	$^1A'$	−642.376861	33.48
3q	$C_7F_3^-$	C_s	$^1A'$	−566.127081	79.15	5g	$C_9F_3^-$	C_s	$^1A'$	−642.371549	36.81
3r	$C_7F_3^-$	C_s	$^3A''$	−566.109243	90.34	5h	$C_9F_3^-$	C_s	$^1A'$	−642.371683	36.73
3s	$C_7F_3^-$	C_s	$^3A'$	−566.099774	96.29	5i	$C_9F_3^-$	C_s	$^1A'$	−642.367496	39.36
3t	$C_7F_3^-$	C_s	$^3A'$	−566.098309	97.21	5j	$C_9F_3^-$	C_s	$^1A'$	−642.366601	39.92
4a	$C_8F_3^-$	C_s	$^1A'$	−604.318782	0.00	5k	$C_9F_3^-$	C_s	$^3A''$	−642.362534	42.47
4b	$C_8F_3^-$	C_s	$^1A'$	−604.311126	4.73	5l	$C_9F_3^-$	C_{2v}	$^1A_1$	−642.349597	50.59
4c	$C_8F_3^-$	C_s	$^3A''$	−604.311247	4.80	5m	$C_9F_3^-$	C_s	$^3A''$	−642.349195	50.84
4d	$C_8F_3^-$	C_s	$^1A'$	−604.302659	10.12	5n	$C_9F_3^-$	C_s	$^1A'$	−642.344210	53.97
4e	$C_8F_3^-$	C_s	$^1A'$	−604.301919	10.58	5o	$C_9F_3^-$	C_s	$^1A'$	−642.340458	56.32
4f	$C_8F_3^-$	C_s	$^1A'$	−604.299951	11.82	5p	$C_9F_3^-$	C_s	$^3A''$	−642.339943	56.64
4g	$C_8F_3^-$	C_s	$^1A'$	−604.299724	11.96	5q	$C_9F_3^-$	C_s	$^1A'$	−642.338647	57.46
4h	$C_8F_3^-$	C_{2v}	$^1A_1$	−604.296889	13.74	5r	$C_9F_3^-$	C_s	$^1A'$	−642.338151	57.77
4i	$C_8F_3^-$	C_s	$^1A'$	−604.286742	20.11	5s	$C_9F_3^-$	C_s	$^1A'$	−642.335366	59.52
4j	$C_8F_3^-$	C_{2v}	$^1A_1$	−604.284434	21.55	5t	$C_9F_3^-$	C_s	$^1A'$	−642.331648	61.85

3.2. Bonding character

Displayed in Fig. 6 are the bond lengths, NBO charges, and bond orders of the G-S $C_nF_3^-$ (n = 1–9) clusters. One can see that the C–F lengths are within the 1.331–1.450 Å range, exhibiting essentially characteristic of single bond. It has been pointed out by Van Orden and Saykally that the bonding of short linear carbon chains could be either cumulene- or polyacetylene-like [1]. Along the C_n chains of G-S $C_nF_3^-$ (n = 3–9), we find that the length of the C–C bonds show an alternate short/long pattern. When n is odd, the C–C bonds display character typical of polyacetylene, i.e., a series of alternate triple and single bonds with lengths falling, respectively, into the 1.221–1.263 and 1.325–1.432 Å range. When n is even (with n = 6 being exceptional), the C_n chains also show polyacetylene-like character, only that the C_2F_3 units are with C=C bonding (1.335–1.343 Å). As an illustration, the bond lengths of G-S $C_8F_3^-$ and $C_9F_3^-$ versus the number of bond (as counted from the left side of chains in Fig. 6) are depicted in Fig. 7. Furthermore, the results of Gaussian NBO based on natural bond orbitals analysis corroborate the above bonding characteristics. The results show that all the C–F bonds are single bonds; when n is odd, the C_n chains display alternate triple and single bonds (i.e., polyacetylene-like), when n is even, the C_n chains are also polyacetylene-like but with the C–C of the C_2F_3 unit being a double bond. The bond orders of the G-S $C_nF_3^-$ (n = 1–9) clusters shown in Fig. 6 are results of direct NBO calculations.

As for the G-S $C_6F_3^-$ isomer, the main structure is a planar C_6 ring (Model 2a). In some cases of NaC_n^- and MgC_n^- clusters, the G-S isomers are cyclic rather than linear [30–32]. The p_z orbitals of the six carbon atoms of Model 2a overlap, and the six π electrons delocalize to form a cyclic π bond. The p_z orbitals of the three fluorine atoms overlap with the cyclic π bond, resulting in reduction

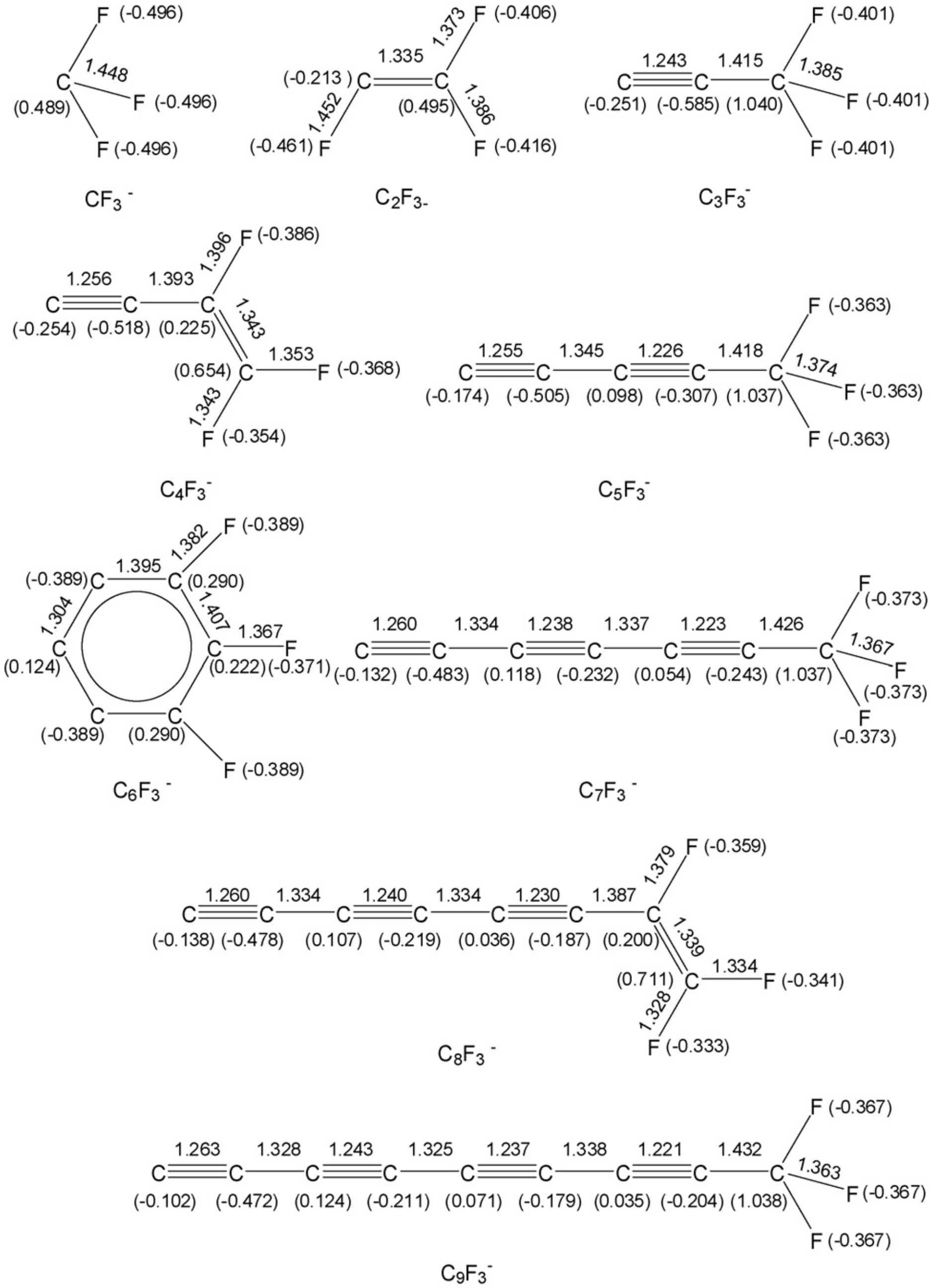

Fig. 6. Bond lengths (Å), NBO charges (in parentheses), and bond orders (line number between two atoms) of the G-S $C_nF_3^-$ (n = 1–9) clusters.

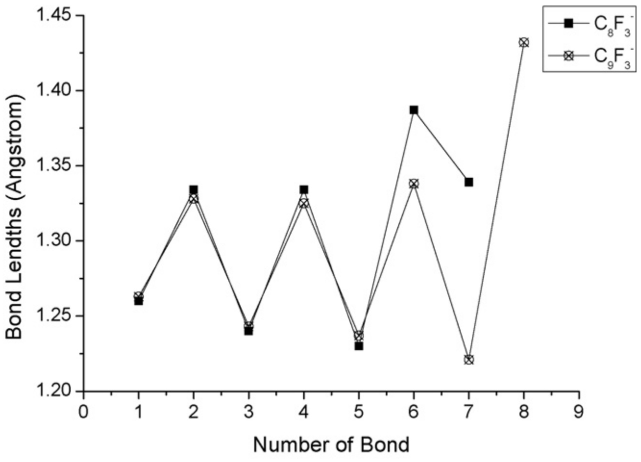

Fig. 7. Bond lengths (Å) of the G-S $C_8F_3^-$ and $C_9F_3^-$ clusters versus the number of bond (as counted from the left side of chains in Fig. 6).

of total energy. In Fig. 8, the π molecular orbital of 3D isosurface of G-S $C_6F_3^-$ is depicted schematically.

According to the NBO charges shown in Fig. 6, the majority of negative charge is located on the fluorine atoms (in the range of −0.333 to −0.496). It is understandable because fluorine is higher than carbon in electronegativity. The rest of the negative charge is distributed in the C_n chain, with the two carbon atoms at the other end of the chain showing higher level of negative charge. It is known that a distribution of negative charges at the two ends of a chain may reduce Coulomb repulsion force, and hence better structure stability [50].

3.3. *Vertical electron detachment energy*

Vertical electron detachment energy (*VDE*) defined as the energy required to remove an electron from an anion but without any geometric change, can be used to evaluate the relative stability of anionic clusters of different sizes. *VDE* can be expressed as [51]:

$$VDE = E(\text{neutral at optimized anion geometry}) - E(\text{optimized anion}).$$

Listed in Table 3 are the *VDE* and incremental binding energy (ΔE^I) of G-S $C_nF_3^-$ ($n = 2$–9) whereas Fig. 9 depicts the *VDE* values versus the number of carbon atoms in G-S $C_nF_3^-$ ($n = 2$–9). There is an obvious parity effect on the *VDE* curve: the *VDE* of odd-*n* clusters are higher than those of adjacent even-*n* cluster(s). The results suggest that the odd-*n* $C_nF_3^-$ clusters are more stable than the neighboring even-*n* ones. This behavior reflects the higher stability of odd-*n* $C_nF_3^-$ ($n = 2$–9) clusters.

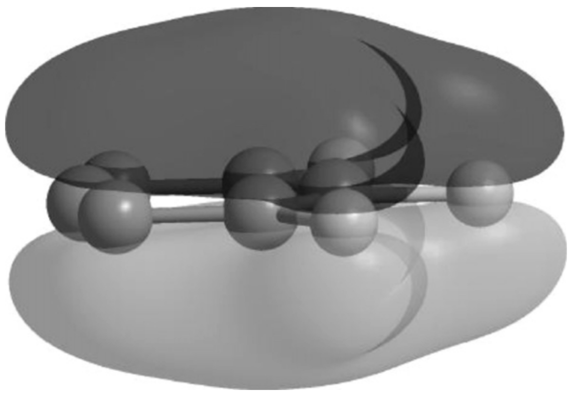

Fig. 8. Schematic of π molecular orbital of 3D isosurface of G-S $C_6F_3^-$.

Table 3
Vertical electron detachment energy *VDE* (a.u.), and incremental binding energy ΔE^I (a.u.) of the G-S $C_nF_3^-$ ($n = 2$–9).

Clusters	*VDE*	ΔE^I
$C_2F_3^-$	0.132918	0.197709
$C_3F_3^-$	0.165945	0.263531
$C_4F_3^-$	0.133631	0.201885
$C_5F_3^-$	0.165302	0.257805
$C_6F_3^-$	0.145377	0.225112
$C_7F_3^-$	0.159657	0.234887
$C_8F_3^-$	0.144258	0.205950
$C_9F_3^-$	0.158998	0.254163

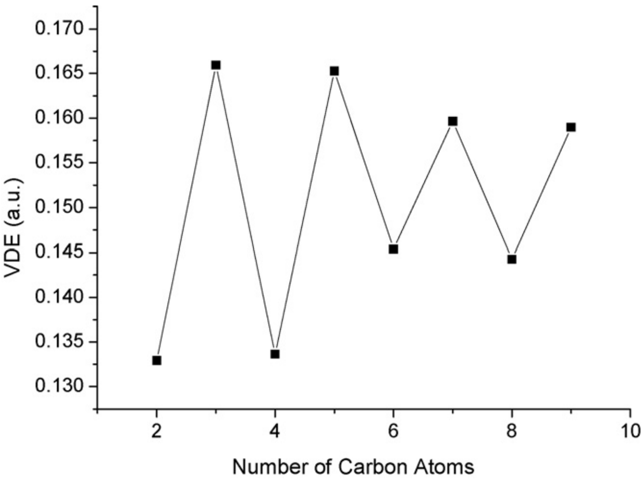

Fig. 9. Vertical electron detachment energy *VDE* (a.u.) of the G-S $C_nF_3^-$ ($n = 2$–9) clusters (as shown in Table 3).

3.4. *Incremental binding energy*

The incremental binding energy (ΔE^I) which is the atomization energy difference (ΔE_a) of adjacent clusters can reflect the relative stability of anionic clusters [52]. It is expressed as

$$\Delta E^I = \Delta E_a(C_nF_3^-) - \Delta E_a(C_{n-1}F_3^-),$$

where ΔE_a is defined as the energy difference between a molecule and its component atoms [47].

As shown in Fig. 10, the values of ΔE^I vary according to a pattern of odd/even alternation: when *n* is odd, the ΔE^I value is big whereas

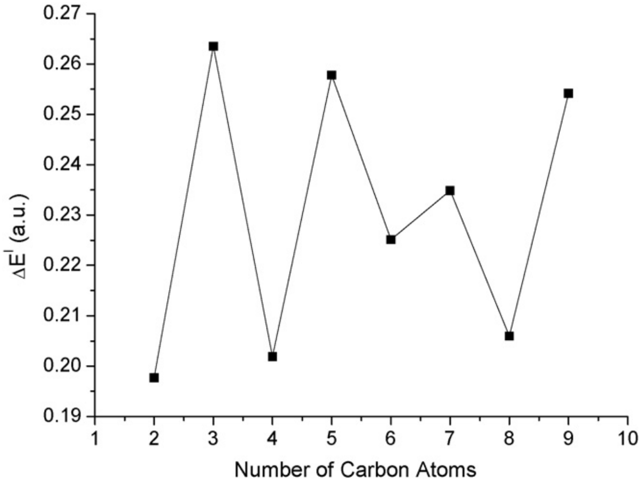

Fig. 10. Incremental binding energies ΔE^I (a.u.) of the G-S $C_nF_3^-$ ($n = 2$–9) clusters (as shown in Table 3) versus *n*.

when n is even, the ΔE^I is small. Because a larger ΔE^I value implies a more stable $C_nF_3^-$ structure, one can deduce that a $C_nF_3^-$ cluster with odd n is more stable than one with even n. Such odd/even alternate pattern of *VDE* and incremental binding energy is consistent with the experimental observation of Gnaser using a standard secondary-ion mass spectrometer [10].

4. Conclusion

When n is odd, the G-S isomers of $C_nF_3^-$ ($n = 3$–9) are with the three fluorine atoms bonded to an end atom of the linear C_n chain. The carbon atoms of G-S $C_2F_3^-$ isomer are sp^2 hybridized, giving a planar $FC{=}CF_2$ structure. For G-S $C_4F_3^-$ and $C_8F_3^-$, the C_4 and C_8 chain are bent, displaying a C_2F_3 unit with structure similar to that of G-S $C_2F_3^-$ at one end. The G-S $C_6F_3^-$ isomer is with the three fluorine atoms bonded to the three carbon atoms at one side of a planar C_6 ring. For the carbon chains with odd or even number of carbon atoms, the bond lengths and bond orders suggest a polyacetylene-like structure. The odd-n anionic clusters are more stable than the adjacent even-n ones. The trend of odd/even alternation can be observed in the variation of bond length, vertical electron detachment energy, and incremental binding energy. The results of calculation are in good agreement with the relative intensity of the $C_nF_3^-$ species observed in mass spectrometric studies. In the synthesis of carbon clusters doped with three fluorine atoms, the molecules with a pyramidal CF_3 unit bonded to an end of a linear carbon chain would be the most favorite. When there is a rise in the number of carbon atoms, the clusters with the fluorine atoms bonded to the atoms of a carbon ring structure would be preferred. Under suitable conditions, the configurations could be the popular structures of carbon clusters richly doped with fluorine atoms.

Acknowledgements

This work was supported by the National Science Foundation of China (grants 20873107 and 20533020).

References

[1] A. Van Orden, R.J. Saykally, Chem. Rev. 98 (1998) 2313.
[2] W. Weltner Jr., R.J. Van Zee, Chem. Rev. 89 (1989) 1713.
[3] N. Moazzen-Ahmadi, F. Zerbetto, J. Chem. Phys. 103 (1995) 6343.
[4] S.N. Khanna, P. Jena, Chem. Phys. Lett. 336 (2001) 467.
[5] S. Becker, H.J. Dietze, Int. J. Mass Spectrom. Ion Process. 82 (1988) 287.
[6] D. Consalvo, A. Mele, D. Stranges, A. Giardini-Guidoni, R. Teghil, Int. J. Mass Spectrom. Ion Process. 91 (1989) 319.
[7] R.B. Huang, C.R. Wang, Z.Y. Liu, L.S. Zheng, F. Qi, L.S. Sheng, S.Q. Yu, Y.W. Zhang, Z. Phys. D: Atom Mol. Clust. 33 (1995) 49.
[8] M. Leleyter, P. Joyes, Surf. Sci. 156 (1985) 800.
[9] R.G. Orth, H.T. Jonkman, J. Michl, Int. J. Mass Spectrom. Ion Phys. 43 (1982) 41.
[10] H. Gnaser, Nucl. Instrum. Methods Phys. Res. B 212 (2003) 407.
[11] C.R. Wang, R.B. Huang, Z.Y. Liu, L.S. Zheng, Chem. Phys. Lett. 237 (1995) 463.
[12] C.-R. Wang, R.-B. Huang, Z.-Y. Liu, L.-S. Zheng, Chem. Phys. Lett. 242 (1995) 355.
[13] Z.Y. Liu, R.B. Huang, L.S. Zheng, Chem. J. Chin. Univ. 18 (1997) 2019.
[14] Z.Y. Liu, R.B. Huang, Z.C. Tang, L.S. Zheng, Chem. Phys. 229 (1998) 335.
[15] H.Y. Wang, R.B. Huang, H. Chen, M.H. Lin, L.S. Zheng, J. Phys. Chem. A 105 (2001) 4653.
[16] C.G. Zhan, S. Iwata, J. Chem. Phys. 104 (1996) 9058.
[17] C.G. Zhan, S. Iwata, J. Phys. Chem. A 101 (1997) 591.
[18] C.G. Zhan, S. Iwata, J. Chem. Phys. 107 (1997) 7323.
[19] G. Pascoli, H. Lavendy, Chem. Phys. Lett. 312 (1999) 333.
[20] G. Pascoli, H. Lavendy, J. Phys. Chem. A 103 (1999) 3518.
[21] K. Fisher, I. Dance, G. Willet, Eur. Mass Spectrom. 3 (1997) 331.
[22] G. Li, Z. Tang, J. Phys. Chem. A 107 (2003) 5317.
[23] G. Li, X. Xing, Z. Tang, J. Chem. Phys. 118 (2003) 6884.
[24] Y. Cao, G. Li, Z. Tang, Chin. Sci. Bull. 50 (2005) 845.
[25] R. Vandenbosch, D.I. Will, J. Chem. Phys. 104 (1996) 5600.
[26] S. Hunsicker, R.O. Jones, J. Chem. Phys. 105 (1996) 5048.
[27] M. Gomei, R. Kishi, A. Nakajima, S. Iwata, K. Kaya, J. Chem. Phys. 107 (1997) 10051.
[28] L. Pan, B.K. Rao, A.K. Gupta, G.P. Das, P. Ayyub, J. Chem. Phys. 119 (2003) 7705.
[29] P. Redondo, C. Barrientos, A. Largo, Int. J. Quantum Chem. 96 (2004) 615.
[30] P. Redondo, C. Barrientos, A. Cimas, A. Largo, J. Phys. Chem. A 108 (2004) 212.
[31] P. Redondo, C. Barrientos, A. Cimas, A. Largo, J. Phys. Chem. A 107 (2003) 6317.
[32] P. Redondo, C. Barrientos, A. Cimas, A. Largo, J. Phys. Chem. A 107 (2003) 4676.
[33] P. Redondo, C. Barrientos, A. Largo, J. Phys. Chem. A 108 (2004) 11132.
[34] A. Largo, A. Cimas, P. Redondo, C. Barrientos, Int. J. Quantum Chem. 84 (2001) 127.
[35] L. Largo, A. Cimas, P. Redondo, V.M. Rayon, C. Barrientos, Int. J. Mass Spectrom. 266 (2007) 50.
[36] P. Redondo, C. Barrientos, A. Largo, Int. J. Mass Spectrom. 263 (2007) 101.
[37] H.J. Zhai, L.S. Wang, P. Jena, G.L. Gutsev, C.W. Bauschlicher Jr., J. Chem. Phys. 120 (2004) 8996.
[38] J.W. Liu, M.D. Chen, L.S. Zheng, Q.E. Zhang, C.T. Au, J. Phys. Chem. A 108 (2004) 5704.
[39] M.D. Chen, X.B. Li, J. Yang, Q.E. Zhang, C.T. Au, Int. J. Mass Spectrom. 253 (2006) 30.
[40] J.Y. Qi, L. Dang, M.D. Chen, W. Wu, Q.E. Zhang, C.T. Au, J. Phys. Chem. A 112 (2008) 12456.
[41] J. Yang, J.Y. Qi, J. Liu, M.D. Chen, Q.E. Zhang, C.T. Au, Int. J. Mass Spectrom. 272 (2008) 172.
[42] Hypercube Inc., HyperChem Reference Manual, Waterloo, Ont., Canada, 1996.
[43] M.J. Frisch, G.W. Trucks, H.B. Schlegel, G.E. Scuseria, M.A. Robb, J.R. Cheeseman, J. Montgomery, J.A.T. Vreven, K.N. Kudin, J.C. Burant, J.M. Millam, S.S. Iyengar, J. Tomasi, V. Barone, B. Mennucci, M. Cossi, G. Scalmani, N. Rega, G.A. Petersson, H. Nakatsuji, M. Hada, M. Ehara, K. Toyota, R. Fukuda, J. Hasegawa, M. Ishida, T. Nakajima, Y. Honda, O. Kitao, H. Nakai, M. Klene, X. Li, J.E. Knox, H.P. Hratchian, J.B. Cross, V. Bakken, C. Adamo, J. Jaramillo, R. Gomperts, R.E. Stratmann, O. Yazyev, A.J. Austin, R. Cammi, C. Pomelli, J.W. Ochterski, P.Y. Ayala, K. Morokuma, G.A. Voth, P. Salvador, J.J. Dannenberg, V.G. Zakrzewski, S. Dapprich, A.D. Daniels, M.C. Strain, O. Farkas, D.K. Malick, A.D. Rabuck, K. Raghavachari, J.B. Foresman, J.V. Ortiz, Q. Cui, A.G. Baboul, S. Clifford, J. Cioslowski, B.B. Stefanov, G. Liu, A. Liashenko, P. Piskorz, I. Komaromi, R.L. Martin, D.J. Fox, T. Keith, M.A. Al-Laham, C.Y. Peng, A. Nanayakkara, M. Challacombe, P.M.W. Gill, B. Johnson, W. Chen, M.W. Wong, C. Gonzalez, J.A. Pople, Gaussian 03 (Revision D.01), Gaussian, Inc., Wallingford, CT, 2004.
[44] A.D. Becke, J. Chem. Phys. 98 (1993) 5648.
[45] C. Lee, W. Yang, R.G. Parr, Phys. Rev. B: Condens. Matter 37 (1988) 785.
[46] W.J. Hehre, L. Radom, R.V.R. Schleyer, J.A. Pople, Ab Initio Molecular Orbital Theory, Wiley-Interscience, New York, 1986.
[47] J.B. Foresman, A. Frisch, Exploring Chemistry with Electronic Structure Methods, Gaussian, Inc., Pittsburgh, PA, 1996.
[48] K. Chuchev, J.J. BelBruno, J. Phys. Chem. A 108 (2004) 5226.
[49] A. Dreuw, L.S. Cederbaum, J. Chem. Phys. 111 (1999) 1467.
[50] A. Dreuw, L.S. Cederbaum, Chem. Rev. 102 (2002) 181.
[51] J.C. Rienstra-Kiracofe, G.S. Tschumper, H.F. Schaefer III, S. Nandi, G.B. Ellison, Chem. Rev. 102 (2002) 231.
[52] G. Pascoli, H. Lavendy, Int. J. Mass Spectrom. Ion Process. 173 (1998) 41.